

β decay of ^{95}Ag

S. Harissopulos,¹ J. Döring,² M. La Commara,^{2,3} K. Schmidt,² C. Mazzocchi,^{2,4} R. Borcea,^{2,4} S. Galanopoulos,¹ M. Górski,² H. Grawe,² M. Hellström,² Z. Janas,^{2,5} R. Kirchner,² E. Roeckl,² I. P. Johnstone,⁶ R. Schwengner,⁷ and L. D. Skouras¹

¹*Institute of Nuclear Physics, NCSR “Demokritos,” GR-153.10 Aghia Paraskevi, Athens, Greece*

²*Gesellschaft für Schwerionenforschung mbH, GSI, Planckstrasse 1, D-64291 Darmstadt, Germany*

³*Università di Napoli “Federico II” and INFN, I-80126 Naples, Italy*

⁴*Università degli Studi di Milano, I-20133 Milan, Italy*

⁵*Institute of Experimental Physics, Warsaw University, PL-00681 Warsaw, Poland*

⁶*Department of Physics, Queen’s University, Kingston, Ontario, Canada, K7L 3N6*

⁷*Institut für Kern- und Hadronenphysik, Forschungszentrum Rossendorf e.V., D-01314 Dresden, Germany*

(Received 26 April 2005; published 10 August 2005)

We studied the β -decay properties of the $N = Z + 1$ nucleus ^{95}Ag by measuring β -delayed γ rays and β - γ - γ coincidences with a plastic scintillator as β detector and a Ge-detector array. The ^{95}Ag nuclei were produced by means of the $^{58}\text{Ni}(^{40}\text{Ca}, p2n)$ reaction and separated with the GSI online mass separator. The previously reported level scheme of the ^{95}Pd daughter nucleus was extended considerably. The deduced level scheme is compared with different shell-model calculations with or without breaking the ^{100}Sn core.

DOI: [10.1103/PhysRevC.72.024303](https://doi.org/10.1103/PhysRevC.72.024303)

PACS number(s): 23.40.Hc, 21.60.Cs, 23.20.Lv, 27.60.+j

I. INTRODUCTION

Proton-rich nuclei in the vicinity of the doubly magic nucleus ^{100}Sn provide a proper testing ground for the nuclear shell model. In this region the valence nucleons outside the doubly magic $Z = N = 50$ core are very few, and therefore large-scale shell-model calculations are feasible. So far, numerous experimental works have been carried out along the $N = Z$ line below ^{100}Sn or close to it. Such nuclei raised interest because of the relevance of their structure to astrophysics: Data on properties like lifetimes, nuclear masses, $\log(ft)$ values, and proton separation energies of nuclei near the proton dripline are necessary for carrying out network calculations within the modeling of the rapid hydrogen-burning process, frequently termed the rp process [1]. This process is proposed to contribute to the nucleosynthesis of certain proton-rich nuclei with masses up to $A \approx 100$ occurring in very hot and dense stellar environments like, e.g., an x-ray burster.

In addition to the astrophysical motivation, there is a twofold nuclear-structure interest in $N \approx Z$, like ^{100}Sn and its neighbors. First, these nuclei are characterized by phenomena such as β decay with a large Q value, β -delayed proton emission, and spin-gap isomers. Second, they provide excellent conditions for the study of the residual proton-neutron interaction in identical orbits ($\pi\nu$ pairing) and the role of core excitations. The study of, e.g., β -decaying spin-gap isomers is of key importance for testing shell-model predictions. The observation of such a β -decaying $21/2^+$ isomer in ^{95}Pd by Nolte and Hick [2,3], the first one reported in the $Z \approx N \approx 50$ region, has initiated a series of β -decay studies in the silver isotopes at the GSI online mass separator [4–6]. In particular, the β decay of ^{95}Ag ($Z = 47$, $N = 48$) has been investigated by Schmidt *et al.*, who established a level scheme consisting of four excited states up to ≈ 2 MeV for the ^{95}Pd daughter nucleus by measuring initially β -delayed protons [5] and then β -delayed γ rays [6]. The allowed Gamow-Teller β decay of the $(9/2^+)$ ground state of ^{95}Ag is expected to be characterized

by two disintegration modes, namely one populating the $(9/2^+)$ ground state of ^{95}Pd and one feeding high-lying $7/2^+$, $9/2^+$, and $11/2^+$ levels in ^{95}Pd , which form the single-particle Gamow-Teller resonance. In the latter case, high-resolution γ spectroscopy faces the problem that a major part of the β intensity usually remains unobserved (see, e.g. Ref. [7]).

Recently, two high-spin isomers were found in ^{95}Ag . The first one, suggested as a $J^\pi = 23/2^+$ isomer, has been observed by in-beam [8] and β -decay [9] studies. This high-spin isomer, whose experimental excitation energy is 2.53 MeV, was predicted by Ogawa [10] 20 years ago. The second high-spin isomer in ^{95}Ag , which was reported in [9], is most probably a $J^\pi = 37/2^+$ level at an excitation energy of 4.86 MeV. It is worth mentioning that the results of [9] were based on the analysis of γ - γ coincident events being vetoed by the detections of positrons (anti- β - γ - γ coincidences). The present work is the continuation of Ref. [6]. It reports on a recent investigation of the β decay of ^{95}Ag that was carried out with a composite Ge detector array with a γ -ray efficiency considerably higher than that reported in Ref. [6].

II. EXPERIMENTAL PROCEDURES AND SETUP

The present measurements were carried out at the GSI online mass separator. The ^{95}Ag nuclei were produced by means of the $^{58}\text{Ni}(^{40}\text{Ca}, p2n)$ reaction with a ^{40}Ca beam of 3.9 MeV/u and 80 particle-nA from the UNILAC accelerator. A 2.7-mg/cm²-thick Nb foil was used as beam degrader in front of the target, which was 2.8 mg/cm² thick and 99.9% enriched ^{58}Ni . The reaction products were stopped in a hot carbon catcher inside a FEBIAD-B2C ion source. After ionization and extraction from the source, the mass-95 secondary beam was separated by a magnetic field and implanted into a transport tape. The decay of the mass-95 activity was measured during implantation cycles of 4.8 s with the detector setup that is described further on in the text. The subsequent implantation

cycle was started 120 ms later. During this period the data acquisition system was stopped and the implantation point of the tape was transported to a properly shielded position within 113 ms. The total measuring time was ≈ 7.5 h. The intensity of the mass-separated ^{95}Ag beam was 28 atoms/s. This was derived from the γ intensity of the 1262-keV γ transition assigned to the $^{95}\text{Ag} \rightarrow ^{95}\text{Pd}$ decay [6].

The implantation position was surrounded by 13 Ge crystals in close geometry. Seven of them were arranged in a Cluster and four in a Clover detector, whereas the remaining ones were a single Ge detector having a relative efficiency of 60% and a low-energy photon spectrometer. The absolute photopeak efficiency determined by means of calibration sources of ^{60}Co , ^{88}Y , ^{109}Cd , ^{137}Cs , and ^{241}Am was 3.5% at an energy of 1.33 MeV. The β particles were detected with a plastic scintillator having a β -detection efficiency of about 85%, as deduced from a ^{22}Na source. A photo of the setup used is given in Ref. [11].

III. DATA ANALYSIS AND EXPERIMENTAL RESULTS

In the present work, single as well as coincidence events were stored on a magnetic tape for offline analysis. The spectrum of the γ rays measured in coincidence with β particles is shown in Fig. 1. Table I lists the energies of β -delayed γ rays assigned to ^{95}Ag and their intensities, obtained in this work, as well as half-life data taken from [6] and γ - γ coincidence relationships discussed in the following text. The strong 511-keV line occurring in the spectrum displayed in Fig. 1 may partly stem from the β decay of ^{95}Ag to the ground state of ^{95}Pd , mentioned in Sec. I. However, because of contributions from isobaric contaminants, we have not performed a quantitative analysis of the intensity of this disintegration branch.

In the offline analysis, standard β - γ coincidence matrices ($4k \times 4k$) were sorted for all Ge-Ge combinations. Various γ - γ coincidence spectra were obtained by the setting of gates on γ transitions of interest and on proper background regions. The latter spectra were subsequently subtracted from the former ones to obtain background-corrected γ - γ coincidence spectra, some of which are plotted in Fig. 2. The γ spectrum shown in part a of Fig. 2 was obtained by gating on the 1262-keV γ transition, which was assigned in Ref. [6] to the $^{95}\text{Ag} \rightarrow ^{95}\text{Pd}$ decay. Panels b–d of Fig. 2 display the γ spectra derived by gating on the 1351-, 1686- and 2025-keV γ transitions, respectively. The latter two gating transitions have also been assigned in Ref. [6] to the $^{95}\text{Ag} \rightarrow ^{95}\text{Pd}$ decay.

The spectrum plotted in Fig. 2(a) includes the 539-keV γ ray found [6] in mutual coincidence with the gating transition as well as some other γ transitions that are explicitly labeled with their energies. From the latter transitions, the 89-keV one was reported in Ref. [8] to be in coincidence with the 1262-keV γ ray, whereas the remaining coincident lines (see Table I) were first observed in the present work. To demonstrate the mutual coincidence relationship between the 1262-keV γ ray and the 89-keV γ transition, part of the γ spectrum obtained by gating on the latter γ ray is shown in insert (I) of Fig. 2. For the same reasons, inserts (II)–(IV) were included in panels b–d of

TABLE I. Energies E_γ , relative intensities I_γ normalized to the 1262-keV γ ray, and coincidence relationships of the γ transitions observed in ^{95}Pd after the β decay of ^{95}Ag . The listed half-lives $T_{1/2}$ were taken from Ref. [6]. The relative intensities were determined from the β -gated γ spectrum, disregarding summing corrections. Energies given in parenthesis indicate uncertain coincidence relationships.

E_γ (keV)	I_γ (%)	$T_{1/2}$ (s)	Coincident γ transitions
89.3(7) ^a	1.6(9)		511, 1220, 1262
539.0(1)	13.9(11)		488, ^b 511, (605), 1262
580.8(2)	6.3(8)		511, 1686
597.5(2)	3.8(11)		511, 1686
605.1(2)	3.8(6)		511, 539, 1262, 1423 ^b
621.9(2)	5.2(8)		511, 761, 1351
675.7(2)	12(1)		511, 2025
720.0(2)	2.3(5)		511, 1686
763.1(2)	3.1(6)		511, 1262
802.1(2)	5.7(8)		511, 1686
1014.7(2)	9.1(11)		511, 1686
1021.7(2)	14.9(13)		511, 1262
1219.6(2)	58(3)		511, 1351
1226.2(2)	3.4(7)		511, 1262
1254.1(2)	5.9(9)		511, 1686
1261.8(1)	100(5)	1.82(23)	89, 511, 539, (605), 763, 1022, 1226, 1472
1351.1(1)	121(7) ^c		511, 622, 1220
1384.0(3)	5.8(9)		511, 2025
1471.7(3)	4.3(8)		511, 1262
1686.0(1)	60(4)	1.73(20)	511, 581, 598, 720, 802, 1015, 1254
1800.6(2)	13.4(12)		511
2024.9(1)	44(3)	1.73(29)	511, 676, (1384)
2570.8(2)	9.3(11)		511
2940.2(2)	10.2(12)		511

^aThe energy and the intensity of this line are rather uncertain because of the nonlinear energy response of the analog-to-digital converter below 100 keV and a possible intensity contribution from the neighboring 87.3-keV x ray of Pb.

^b γ transition not placed in the level scheme.

^cDoublet line observed ^{95}Pd and in ^{95}Rh . The intensity value given includes both components.

Fig. 2. These inserts show parts of the background-corrected γ spectra obtained by setting gates on the 1220-, 802-, and 676-keV γ rays, respectively. The coincident γ transitions included in parts c and d were observed for the first time in the present work.

The 1351-keV γ ray was first assigned by Kurcewicz *et al.* [4] to the $^{95m}\text{Pd} \rightarrow ^{95}\text{Rh}$ β decay. Indeed, as shown in part b of Fig. 2, the γ spectrum gated on this transition includes the strongest coincident γ transitions reported in Ref. [4]. These are marked here with asterisks. In addition, this spectrum includes a strong 1220-keV γ ray and a weak 622-keV γ transition. The coincidence relation between the former line and the 1351-keV γ ray has already been observed by Schmidt *et al.* [6]. Moreover, the 1220-keV γ ray was found [6] to have a half-life in agreement with those observed for the 1262-, 1686-, and 2025-keV γ transitions but was not assigned [6] to the $^{95}\text{Ag} \rightarrow ^{95}\text{Pd}$ decay because of its coincidence relationship

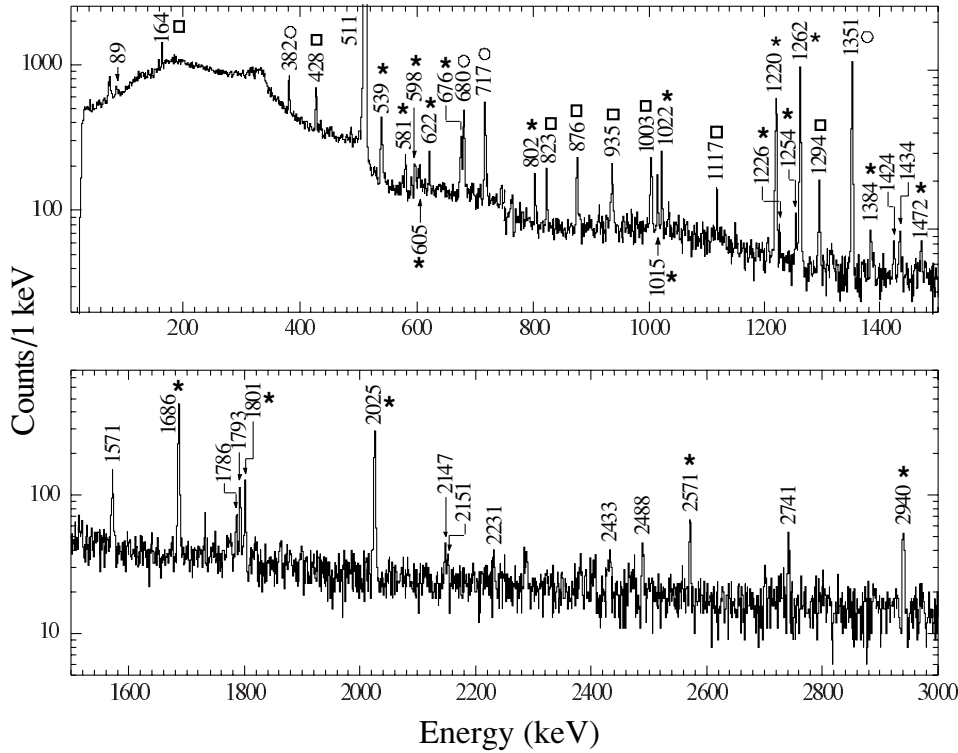


FIG. 1. β -gated γ rays observed in the present work. The strongest γ transitions are labeled with numbers indicating the corresponding photon energy. This spectrum includes (i) almost all γ transitions that according to Refs. [6,9] depopulate excited states of ^{95}Ag , which are labeled with open boxes; (ii) the strongest γ rays reported in Ref. [4] arising from the $^{95m}\text{Pd} \rightarrow ^{95}\text{Rh}$ β decay, marked with open circles; (iii) β -delayed γ transitions deexciting states of ^{95}Pd observed in the present work or in Ref. [6], which are indicated with asterisks, and (iv) β -delayed γ transitions observed in this work that could not definitely be assigned to the decay of ^{95}Pd or ^{95}Ag ; these transitions are not marked with any symbol. Gamma lines deexciting isomeric states of ^{95}Ag may occur in the spectrum because of the conversion electrons detected by the plastic scintillator.

with the 1351-keV γ transition. However, we found evidence of a doublet nature of the latter transition: the observation [8] of the mutual coincidence between the 89-keV γ transition and

the 1262-keV γ -ray, which is confirmed by the present work, proves the existence of a 1351-keV excited state also in ^{95}Pd . As reported in Ref. [8], this level decays directly to the ground

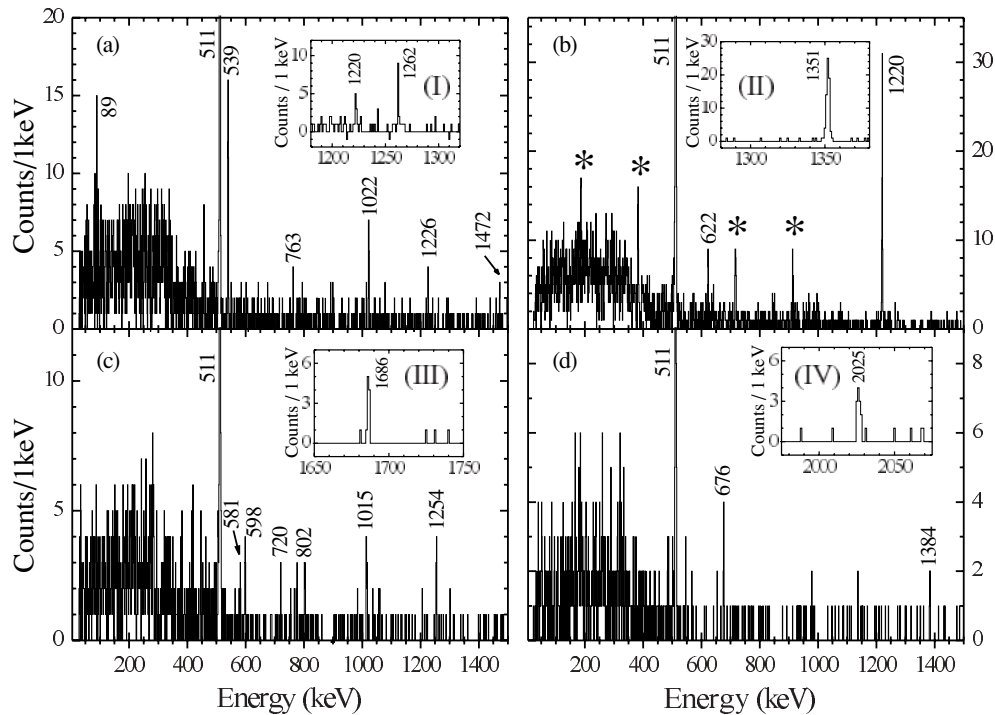


FIG. 2. Background-corrected γ spectra obtained by the setting of gates on the 1262-, 1351-, 1686-, and 2025-keV γ rays. These are shown in parts a–d respectively. The inserts (I)–(IV) show parts of the background-corrected γ spectra derived by gating on the 89-, 1220-, 802-, and 676-keV γ transitions, respectively. The numbers displayed on top of some of the peaks indicate the energies of the corresponding γ transitions in kilo-electron-volts. The asterisks in part b indicate γ rays arising from the $^{95m}\text{Pd} \rightarrow ^{95}\text{Rh}$ β -decay.

state of ^{95}Pd and is populated by a 622-keV γ transition. Hence, all coincidence data shown in panel b of Fig. 2 support the assignment of the 1220- and the 622-keV γ transitions to ^{95}Pd . Moreover, the 1351–622–761-keV cascade establishes the 2734-keV level, with the 1472-keV γ ray connecting this state with the known one [6] at 1262 keV. This means that the ^{95}Pd level schemes from Refs. [6] and [8] are compatible and that the doublet nature of the 1351-keV line [8] is confirmed.

In the present work, the level scheme of ^{95}Pd was constructed with the information compiled in Table I as well as the findings of [6] and [8] taken into account. The resulting level scheme of ^{95}Pd , shown in Fig. 3, consists of 15 excited levels that are depopulated by 25 γ -ray transitions. Four of these levels have already been reported by Schmidt *et al.* [6] whereas two more levels were identified in the recent work of Mărginean *et al.* [8]. Some of the γ transitions displayed in Fig. 3 are drawn with dashed arrows. This indicates that their placement in the level scheme is not definite because the corresponding mutual coincidence relationships are only partly fulfilled.

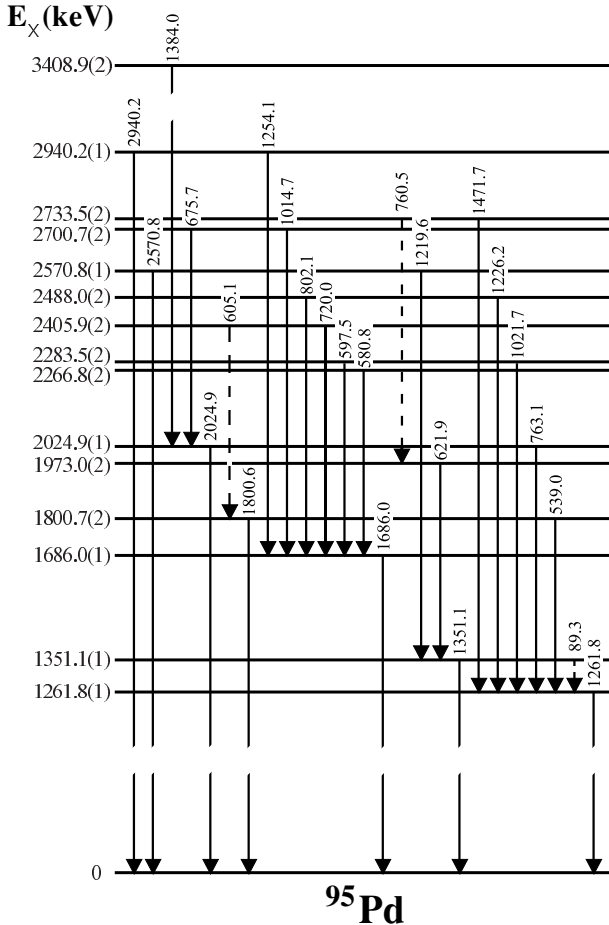


FIG. 3. Level scheme of ^{95}Pd derived in the present work (see also discussion in the text).

TABLE II. Excited states in ^{95}Pd deduced in the present work: the level energies E_x are given in the first column. The intensities I_β of the corresponding apparent β feeding that are given in the second column were deduced from the intensity balance between the respective depopulating and populating γ rays (third and fourth columns, respectively) without any corrections for summing effects and were then normalized to $\Sigma I_\beta = 100\%$.

E_x (keV)	I_β (%)	Depopulating γ rays (keV)	Populating γ rays (keV)
1261.8(1)	20.5(19)	1261.8	89.3, 539.0, 763.1, 1021.7, 1226.2, 1471.7
1351.1(1)	^a	89.3, 1351.1	621.9, 1219.6
1686.0(1)	9.4(16)	1686.0	580.8, 597.5, 720.0, 802.1, 1014.7, 1254.1
1800.7(2)	8.2(6)	539.0, 1800.6	605.1
1973.0(2)	0.9(3)	621.9	
2024.9(1)	6.2(11)	2024.9	675.7, 1384.0
2266.8(2)	2.2(3)	580.8	
2283.5(2)	6.5(6)	597.5, 1021.7	
2406.0(2)	2.0(3)	720.0, 605.1	
2488.0(2)	3.2(4)	802.1, 1226.2	
2570.8(1)	23.4(11)	1219.6, 2570.8	
2700.7(2)	7.4(5)	675.7	
2733.5(3)	2.4(3)	1471.7	
2940.2(2)	5.6(5)	1254.1, 2940.2	
3408.9(2)	2.0(3)	1384.0	

^aNo I_β value is given because the depopulating 1351-keV γ ray is a doublet line.

IV. DISCUSSION

A. The level scheme of ^{95}Pd

The experimental results from this work on excited levels of ^{95}Pd , their depopulating and populating γ transitions, as well as the apparent β -feeding intensities I_β , are listed in Table II. The I_β values result from the intensity differences between depopulating and populating transitions of each excited level without any corrections for summing effects, which were estimated to be of the order of 12–15% at most. These differences were then normalized to yield $\Sigma I_\beta = 100\%$. According to the data given in Table II, the 1262- and 2571-keV states apparently collect most of the β -feeding intensity. On the basis of this observation and their strong direct γ deexcitation to the $(9/2^+)$ ground state of ^{95}Pd , a tentative $(7/2^+, 9/2^+, 11/2^+)$ assignment is proposed for the 1686-, 1801-, and 2571-keV levels, excluding the latter state, but not the one at 2733 keV, as candidates for a daughter state from the β decay of a $23/2^+$ high-spin isomer. All in all, we underline the qualitative character of the discussion based on apparent β intensities. This is due to the problem of missing β intensity in high-resolution γ -ray spectroscopy, mentioned in Sec. I.

An interesting aspect of the level scheme shown in Fig. 3 is the presence of an excited state at 1800.7(1) keV. This state was assigned by summation of the energies of the 1261.8(1) and 539.0(1)-keV γ rays that were found in mutual coincidence, as well as by the observation of a 1800.6(1)-keV γ transition in the β -gated γ spectrum. The intensity of the

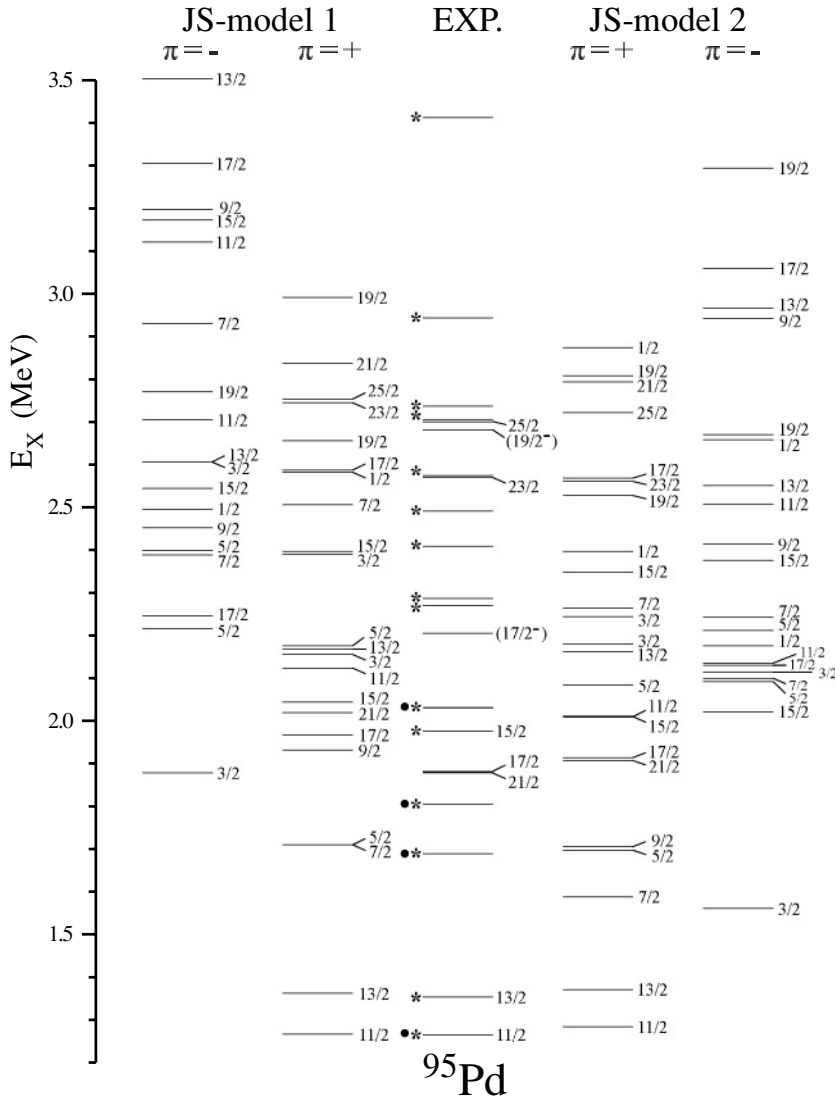


FIG. 4. Comparison of the experimental level scheme of ^{95}Pd (third column) with the results of shell-model calculations made with either JS model 1 (first and second columns) or JS model 2 (fourth and fifth columns). All experimental excited states shown with a spin assignment have been reported in Ref. [8]. Levels observed in the present work are marked with an asterisk, whereas those found in Ref. [6] are marked with a solid circle.

latter γ ray was found to be too strong to be explained by summing only.

B. Shell-model calculations

In the present work two different shell-model calculations are presented. They were performed within two different approaches reported by Johnstone and Skouras [12,13], called hereafter JS model 1 and 2, which are briefly described in the following text.

In JS model 1, an inert ^{100}Sn core is assumed. The valence protons and neutrons are treated as holes occupying the $g_{9/2}$ and $p_{1/2}$ orbitals. An appropriate effective interaction for this model space was obtained as described in Ref. [12]. In JS model 2, which is described in Ref. [13], the ^{100}Sn core is “broken,” i.e., particle-hole excitations are allowed to occur from the $g_{9/2}$ and $p_{1/2}$ orbits to the higher-lying $d_{5/2}$, $s_{1/2}$, $d_{3/2}$, and $g_{7/2}$ shells. As a consequence, the model space is increased considerably and calculations become more complicated because of the exceedingly large dimensions of the relevant energy matrices. On the other hand, the breaking

of the ^{100}Sn core facilitates the theoretical description of the high-spin states. Both models have been tested successfully in many nuclei in the $A \approx 100$ region. In particular, JS model 2 has been found to account successfully for the observed Gamow-Teller distribution in the case of ^{96}Ag [14].

The level scheme of ^{95}Pd including the excited states found in the present work as well as those reported in Ref. [8] up to 3.5 MeV is compared with the predictions of both JS model 1 and 2 calculations in Fig. 4. It has to be emphasized that Fig. 4 does not include the $9/2^+$ ground state as well as the first excited negative-parity states predicted by JS model 1 and 2. The latter states are predicted to have spin 1/2 and excitation energies of 0.816 and 0.560 MeV, respectively. The $1/2^-$ state has not been observed so far. In addition, the maximum spin of the theoretical levels shown in Fig. 4 is 25/2. For each spin the lowest two states have been included, provided that their excitation energy is lower than 3.5 MeV. It has to be emphasized that the spins given in Fig. 4 for some of the experimental levels have not been determined in the present work but they have been adopted from Ref. [8]. Experimental states with no spin assignment have been obtained in the

present work. All observed states for which a spin assignment is given have positive parity, except two cases, i.e. the $(17/2^-)$ and the $(19/2^-)$ state at ≈ 2.2 and ≈ 2.7 MeV, respectively.

As can be seen in Fig. 4, the breaking of the ^{100}Sn core, i.e., JS model 2, shifts most of the levels to lower energies. This effect is most pronounced in the case of the $J^\pi = 3/2^-$ and $J^\pi = 11/2^-$ states. Changes in the spin sequence are also to be seen in Fig. 4. As shown in Fig. 4, both models predict a higher number of excited states than that observed experimentally. A good qualitative agreement between the experimental data and the predictions of both JS models is observed, at least as far as the number of ^{95}Pd levels up to an excitation energy of 3 MeV is concerned. However, for a more sensitive test of the models it is necessary to determine as many as possible spins.

V. SUMMARY

In the present work, the β decay of the $N = Z + 1$ nucleus ^{95}Ag was studied by measurement of β -delayed

γ rays and β - γ - γ coincidences. Seventeen new γ transitions were assigned to the $^{95}\text{Ag} \rightarrow ^{95}\text{Pd}$ decay, and the previously reported level scheme of the ^{95}Pd daughter nucleus was enriched with nine new levels. The comparison of the updated level scheme with two different shell-model calculations with or without breaking the ^{100}Sn core has yielded good qualitative agreement.

ACKNOWLEDGMENTS

The authors thank K. Burkard and W. Hüller for their professional assistance in the operation of the GSI online mass separator. This work was supported in part by the European Community under contract no. HPR-CT-1999-00001 and the Polish Committee of Scientific Research, in particular under grant no. KBN 2 P03B 035 23 and the Program for Scientific Technical Collaboration (WTZ) under project no. POL 99/009.

-
- [1] H. Schatz, A. Aprahamian, J. Görres, M. Wiescher, T. Rauscher, J. F. Rembges, F.-K. Thielemann, B. Pfeiffer, P. Möller, K.-L. Kratz, H. Herndl, B. A. Brown, and H. Rebel, *Phys. Rep.* **294**, 167 (1998).
 - [2] E. Nolte and H. Hick, *Phys. Lett.* **B97**, 55 (1980).
 - [3] E. Nolte and H. Hick, *Z. Phys. A* **305**, 289 (1982).
 - [4] W. Kurcewicz, E. F. Zganjar, R. Kirchner, O. Klepper, E. Roeckl, P. Komninos, E. Nolte, D. Schardt, and P. Tidemand-Petersson, *Z. Phys. A* **308**, 21 (1982).
 - [5] K. Schmidt, Th. W. Elze, R. Grzywacz, Z. Janas, R. Kirchner, O. Klepper, A. Plochocki, E. Roeckl, K. Rykaczewski, L. D. Skouras, and J. Szerypo, *Z. Phys. A* **350**, 99 (1994).
 - [6] K. Schmidt, P. C. Divari, Th. W. Elze, R. Grzywacz, Z. Janas, I. P. Johnstone, M. Karny, H. Keller, R. Kirchner, O. Klepper, A. Plochocki, E. Roeckl, K. Rykaczewski, L. D. Skouras, J. Szerypo, and J. Zylicz, *Nucl. Phys.* **A624**, 185 (1997).
 - [7] Z. Hu, L. Batist, J. Agramunt, A. Algorta, B. A. Brown, D. Cano-Ott, R. Collatz, A. Gadea, M. Gierlik, M. Górski, H. Grawe, M. Hellström, Z. Janas, M. Karny, R. Kirchner, F. Moroz, A. Plochocki, M. Rejmund, E. Roeckl, B. Rubio, M. Shibata, J. Szerypo, J. L. Tain, and V. Wittmann, *Phys. Rev. C* **60**, 024315 (1999).
 - [8] N. Märginean, D. Bucurescu, C. Rossi Alvarez, C. A. Ur, L. D. Skouras, L. P. Johnstone, D. Bazzacco, S. Lunardi, G. de Angelis, M. Axiotis, E. Farnea, A. Gadea, M. Ionescu-Bujor, A. Iordăchescu, W. Krolas, Th. Kröll, S. M. Lenzi, T. Martinez, R. Märginean, R. Menegazzo, D. R. Napoli, P. Pavan, M. De Poli, B. Quintana, C. Rusu, P. Spolaore, and J. Wrzesinski, *Phys. Rev. C* **67**, 061301(R) (2003).
 - [9] J. Döring, H. Grawe, K. Schmidt, R. Borcea, S. Galanopoulos, M. Górski, S. Harissopoulos, M. Hellström, Z. Janas, R. Kirchner, M. La Commara, C. Mazzocchi, E. Roeckl, and R. Schwengner, *Phys. Rev. C* **68**, 034306 (2003).
 - [10] K. Ogawa, *Phys. Rev. C* **28**, R958 (1983).
 - [11] E. Roeckl, A. Blazhev, K. Burkard, J. Döring, H. Grawe, W. Hüller, R. Kirchner, C. Mazzocchi, I. Mukha, and C. Plettner, *Nucl. Instrum. Methods Phys. Res. B* **204**, 53 (2003).
 - [12] I. P. Johnstone and L. D. Skouras, *Eur. Phys. J. A* **11**, 125 (2001).
 - [13] I. P. Johnstone and L. D. Skouras, *Phys. Rev. C* **55**, 1227 (1997).
 - [14] L. Batist, J. Döring, I. Mukha, C. Plettner, C. R. Bingham, R. Borcea, M. Gierlik, H. Grawe, K. Hauschild, Z. Janas, I. P. Johnstone, M. Karny, M. Kavatsyuk, R. Kirchner, M. La Commara, C. Mazzocchi, F. Moroz, J. Pavan, A. Plochocki, E. Roeckl, B. Salvachúa, K. Schmidt, R. Schwengner, L. D. Skouras, S. L. Tabor, and M. Wiedeking, *Nucl. Phys.* **A720**, 245 (2003).